Postprint: Dispersion Characteristics of Scholte Waves Excited by Pulsed and Continuous Acoustic Sources

Authors: Wu Qibiao

Date: 2025-11-01T21:58:41+00:00

Abstract

The dispersion and polarization characteristics of Scholte waves excited by acoustic sources in shallow water are of significant importance for target detection, yet current understanding of Scholte waves generated by impulsive and continuous point sources remains insufficient. This study investigates Scholte waves excited by these two source types using normal mode theory and a time-domain finite element model combined with wavelet transform. First, based on a shallow-water acoustic field model with a semi-infinite elastic seabed, the dispersion characteristics of Scholte waves are analyzed using normal mode theory, demonstrating that dispersion phenomena exist under both hard and soft seabed conditions. Subsequently, the dispersion of Scholte waves and the polarization characteristics of particle motion trajectories excited by impulsive and continuous sources are explored using a time-domain finite element model combined with wavelet transform. The results indicate that, from a time-frequency analysis perspective, Scholte wave dispersion can be observed for both source types in hard seabed environments. For continuous sources, Scholte wave dispersion can be observed in soft seabed conditions, whereas for impulsive sources, the dispersion phenomenon is difficult to observe. Regarding polarization characteristics, the ellipticity of Scholte waves excited by impulsive sources first decreases and then increases, while remaining stable under continuous sources. Scholte waves excited by impulsive sources are dominated by vertical vibration in hard seabed conditions. Scholte waves excited by continuous sources are dominated by vertical vibration in hard seabed conditions and by horizontal vibration in soft seabed conditions. These findings can provide a preliminary basis for detecting impulsive and continuous acoustic sources in shallow water.

Full Text

Preamble

Vol. 42 No. 5

Oct. 2025

Chinese Journal of Applied Mechanics DOI: 10.11776/j.issn.1000-4939.2025.05.019

Research on Dispersion Characteristics of Scholte Waves Excited by Pulsed and Continuous Sound Sources

WU Qibiao[1], CHI Qingjia[1], LIN Yongshui[1], CHEN Wei[2]
(1. School of Science, Wuhan University of Technology, 430070 Wuhan, China;
2. School of Naval Architecture, Ocean and Energy Power Engineering, Wuhan University of Technology, 430070 Wuhan, China)

Abstract: The dispersion and polarization characteristics of Scholte waves excited by sound sources in shallow seas are of great significance for target detection. However, current understanding of Scholte waves excited by pulsed and continuous point sound sources remains insufficient. This study investigates Scholte waves excited by these two types of sources using normal mode theory, time-domain finite element modeling, and wavelet transform. First, based on a shallow-water semi-infinite elastic seabed acoustic field model, the dispersion characteristics of Scholte waves are analyzed using normal mode theory, revealing that dispersion phenomena exist for Scholte waves under both hard and soft seabed conditions. Then, a time-domain finite element model combined with wavelet transform is employed to investigate the dispersion and polarization characteristics of particle motion trajectories for Scholte waves excited by pulsed and continuous sources. The results show that, from a time-frequency analysis perspective, dispersion of Scholte waves can be observed for both source types under hard seabed conditions. For soft seabeds, dispersion can be observed for continuous sources but is difficult to detect for pulsed sources. Regarding polarization characteristics, the ellipticity of Scholte waves excited by pulsed sources first decreases and then increases, whereas it remains stable under continuous excitation. Scholte waves excited by pulsed sources exhibit predominantly vertical vibration under hard seabed conditions. For continuous sources, Scholte waves show vertical vibration under hard seabeds but horizontal vibration under soft seabeds. These findings provide a preliminary basis for detecting pulsed and continuous sound sources in shallow seas.

Keywords: Scholte wave; elastic seabed; dispersion property; polarization property; numerical simulation

Document code: A
Chinese Library Classification: P733.21
Article ID: 1000-4939(2025)05-1165-09

Introduction

With advancements in vibration and noise reduction technology, the radiated noise from ships and underwater vehicles continues to decrease, making their detection and localization increasingly reliant on low-frequency signals. When operating in shallow sea environments, the vibrations, noise, and water disturbances they generate propagate through seawater as pressure waves to the seabed, inducing seismic wave fields that travel along the liquid-solid interface—known as Scholte waves [1]. Compared with primary arrivals and shear waves, Scholte waves attenuate slowly during propagation, making their long-distance propagation characteristics promising for remote target detection.

Understanding Scholte wave characteristics is crucial for target detection applications. Like acoustic waves, Scholte waves carry target position information [2-3], and their phase velocity is key to obtaining such information. Furthermore, seabed shear wave velocity can be inverted through Scholte wave dispersion characteristics [4-5]. Therefore, studying Scholte wave properties is important for both target detection/localization and seabed medium parameter inversion.

Domestic and international scholars have investigated Scholte waves excited by pulsed sound sources through experiments, theoretical analysis, and numerical simulations. Experimentally, Ewing et al. [6] conducted propagation experiments with explosive pulses in shallow water environments and received seafloor seismic waves from underwater explosions, though they did not specifically analyze Scholte wave characteristics. Rauch [7] derived the existence of Scholte waves at the interface between a uniform semi-infinite fluid medium and a semi-infinite elastic medium, and obtained propagation patterns and particle motion trajectories through underwater pulse explosion experiments. Shao et al. [8] used pulsed source experiments to identify Scholte waves extracted via τ-p transform using matching pursuit and Wigner transform, accurately extracting frequency, velocity, and energy parameters, but without further characteristic analysis. Theoretically, Vinh [9] derived the dispersion equation for Scholte waves at fluid half-space and isotropic elastic half-space interfaces using complex function methods, proving their uniqueness. Zhu et al. [10-11] established a semi-infinite elastic seabed Scholte wave model and extended it to layered seabeds, analyzing dispersion characteristics, particle motion trajectories, and displacements. Numerically, Flores-Mendez et al. [12] used the indirect boundary element method to study numerical models of Scholte waves excited by pulsed sources in time and frequency domains, confirming their existence and propagation. Wang et al. [13] established a time-domain numerical calculation model for low-frequency acoustic fields in shallow water full waveguides under pulsed sources, analyzing propagation mechanisms and characteristics. Zhao et al. [14] simulated underwater acoustic fields excited by pulsed sources using LS-DYNA, analyzing excitation mechanisms and particle trajectories, and applied the method to separate Scholte waves from complex wavefield signals.

For Scholte waves excited by continuous sources, Tomar et al. [15] studied ve-

locity tomography of continuously excited Scholte waves, obtaining average dispersion curves through Monte Carlo inversion. Wang et al. [16] verified the accuracy of wave type discrimination and polarization parameter calculation in the time-frequency domain through continuous source experiments and polarization analysis.

Research on particle motion trajectory polarization characteristics of Scholte waves has focused primarily on pulsed sources. Zhao [17] used polarization analysis to distinguish Scholte waves from direct acoustic waves (seismic waves traveling directly from the source to seafloor receivers) in wavefields excited by pulsed sources, then obtained time delay differences using correlation methods to derive target distance information. Lu et al. [18] used polarization analysis to distinguish effective seismic signals from noise. Huang et al. [19] developed a time-frequency domain instantaneous polarization analysis method based on the generalized S-transform, which provides more accurate identification than traditional time-domain methods. Han [20] applied polarization characteristics of ship seismic waves to line spectrum detection for surface vessels, demonstrating significance for long-range detection.

Current research predominantly addresses dispersion and polarization characteristics of Scholte waves excited by pulsed point sources, with insufficient investigation of continuously excited Scholte waves. However, radiated noise from actual underwater targets is primarily continuous. This study establishes a shallow-water semi-infinite elastic seabed Scholte wave model, derives the dispersion equation for shallow seabed Scholte waves based on normal mode theory, and analyzes dispersion characteristics under hard and soft seabed conditions. Time-domain finite element models are applied to simulate Scholte waves excited by both source types, analyzing dispersion and polarization characteristics of particle motion trajectories.

1. Dispersion Characteristics of Shallow Seabed Scholte Waves

A shallow-water layered Scholte wave model is established as shown in [FIGURE:1], where H represents seawater depth, $_1$ is seawater density, c_1 is sound speed in seawater, $_2$ is seabed density, c is longitudinal wave velocity, and c is shear wave velocity. In Cartesian coordinates, ϕ_0 denotes the displacement potential function in the seawater layer, while ϕ_1 and ϕ_2 represent longitudinal and shear wave displacement potential functions in the shallow semi-infinite elastic seabed, respectively.

The displacement potential functions in seawater and elastic seabed satisfy the following wave equations [21]:

$$\frac{\partial^2 \phi_0}{\partial t^2}, \quad \frac{\partial^2 \phi_1}{\partial t^2}, \quad \frac{\partial^2 \phi_2}{\partial t^2}$$

$$\frac{\partial^2\phi_0}{\partial x^2}+\frac{\partial^2\phi_0}{\partial z^2}=\frac{\partial^2\phi_1}{\partial x^2}+\frac{\partial^2\phi_1}{\partial z^2}=\frac{\partial^2\phi_2}{\partial x^2}+\frac{\partial^2\phi_2}{\partial z^2}$$

Since the seawater surface is a pressure-release boundary and the elastic seabed satisfies radiation conditions at infinity, the general solutions for each potential function are:

$$\phi_0 = 2A\sinh(k\xi_1)ze^{i(kx-\omega t)}$$

$$\phi_1 = Be^{-k\xi_l z}e^{i(kx-\omega t)}$$

$$\phi_2 = Ce^{-k\xi_t z}e^{i(kx-\omega t)}$$

where A, B, and C are coefficients for each potential function; = √(1 - c^2/c^2) for i = 1, l, t; $\omega = 2\pi f$; $k = \omega/c$; f is source frequency; and k is wavenumber.

From the relationship between particle displacement and potential functions:

$$w_a=\frac{\partial\phi_0}{\partial x},\quad v_a=\frac{\partial\phi_0}{\partial z},\quad w_b=\frac{\partial\phi_1}{\partial x}+\frac{\partial\phi_2}{\partial z},\quad v_b=\frac{\partial\phi_1}{\partial z}+\frac{\partial\phi_2}{\partial x}$$

where w represents horizontal displacement, v represents vertical displacement, subscript a denotes seawater, and subscript b denotes elastic seabed.

At the liquid-solid interface, boundary conditions require continuity of normal stress and normal displacement, with zero tangential stress [22]:

$$v_a=v_b,\quad \sigma_{zz}^a=\sigma_{zz}^b,\quad \sigma_{xz}^b=0$$

where *σ{zz} represents normal stress and* σ{xz} represents tangential stress.

Stress components expressed in terms of particle displacement are:

$$\sigma_{zz}=\lambda\left(\frac{\partial w}{\partial x}+\frac{\partial v}{\partial z}\right)+2\mu\frac{\partial v}{\partial z}$$

$$\sigma_{xz}=\mu\left(\frac{\partial w}{\partial z}+\frac{\partial v}{\partial x}\right)$$

where λ and are Lamé constants; in seawater $\lambda_1 = {}_1c_1{}^2$, $_1 = 0$; in seabed $\lambda_2 + 2\,{}_2 = {}_2c^2$, $_2 = {}_2c^2$.

Substituting equations (2), (3), and (5) into (4) yields:

$$2\xi_1 A\cosh(k\xi_1)H + \xi_l Be^{-k\xi_l H} - iCe^{-k\xi_t H} = 0$$

$$2\rho_1\omega^2 A\sinh(k\xi_1)H - B\rho_2\omega^2 - 2\rho_{2c}t_t^{2k^{2\xi}}e^{-k\xi_t H} = 0$$

$$2iC\rho_{2c}t^2 - 2i\xi_l Be^{-k\xi_l H} + C(1+\xi_t^2) = 0$$

From these, the characteristic equation is obtained:

$$\left(2-\frac{c^2}{c_t^2}\right)^2 - 4\sqrt{1-\frac{c^2}{c_l^2}}\sqrt{1-\frac{c^2}{c_t^2}} - \frac{\rho_1 c^4}{\rho_2 c_t^4}\frac{\sqrt{1-c^2/c_1^2}}{\sqrt{1-c^2/c_t^2}} = 0$$

This is the dispersion equation for the shallow-water semi-infinite elastic seabed acoustic field model. Numerical calculations are performed for point source-excited Scholte waves under hard and soft seabed conditions, with specific parameters listed in .

1.1 Hard Seabed Medium

Using basalt as a hard seabed medium (c $>$ c) with 50 m water depth, basalt parameters are substituted into dispersion equation (7) to obtain the Scholte wave dispersion curve shown in [FIGURE:2].

[FIGURE:2] shows that seabed seismic waves include Scholte waves and normal modes. Scholte wave velocity decreases with increasing frequency. As source frequency approaches 0 Hz, Scholte wave propagation tends toward Rayleigh waves (waves at air-solid interfaces). Since the tanh term approaches zero, equation (7) reduces to:

$$\left(2-\frac{c^2}{c_t^2}\right)^2 - 4\sqrt{1-\frac{c^2}{c_l^2}}\sqrt{1-\frac{c^2}{c_t^2}} = 0$$

This is the Rayleigh equation, whose solution gives Rayleigh wave velocity—frequency-independent and thus non-dispersive. For source frequencies above 40 Hz, Scholte wave velocity stabilizes with increasing frequency. Here the tanh term approaches 1, and equation (7) becomes:

$$\left(2-\frac{c^2}{c_t^2}\right)^2 - 4\sqrt{1-\frac{c^2}{c_l^2}}\sqrt{1-\frac{c^2}{c_t^2}} - \frac{\rho_1 c^4}{\rho_2 c_t^4} = 0$$

The solution becomes frequency-independent, and Scholte wave propagation approaches Stoneley waves (waves at solid-solid interfaces) without dispersion characteristics.

The figure also shows that first- and second-order normal modes are excited at frequencies above 15 Hz and 39 Hz, respectively, indicating propagating normal modes at the horizontal elastic seabed interface with velocities slower than seabed shear wave speed but faster than seawater sound speed. At cutoff frequencies, velocity approaches seabed shear wave speed, and normal mode velocity also decreases with frequency, demonstrating dispersive behavior.

1.2 Soft Seabed Medium

Using moraine as a soft seabed medium (c $<$ c),

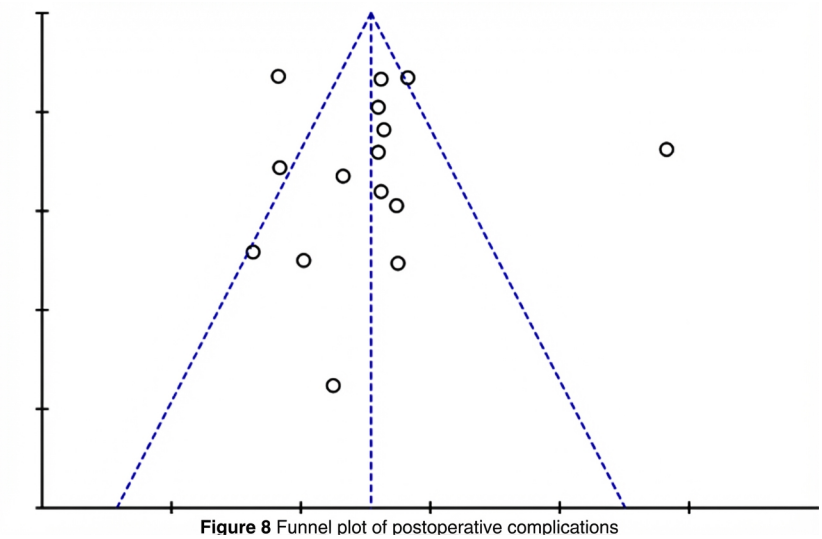

Figure 1: Figure 3

shows the Scholte wave dispersion curve under soft seabed conditions for 50 m water depth. Scholte wave velocity decreases with increasing frequency. As source frequency approaches 0 Hz, velocity tends toward Rayleigh waves, stabilizing for frequencies above 5 Hz. Unlike hard seabeds, no normal mode dispersion occurs in soft seabeds because when phase velocity exceeds shear wave speed, only complex roots exist in the dispersion equation, causing normal modes in seawater and elastic seabed to attenuate with distance. Therefore, normally propagating normal modes do not exist in soft seabeds.

Figures 2 and 3 demonstrate that Scholte waves exhibit dispersion only in very low frequency bands, showing normal dispersion under both hard and soft seabed conditions, with velocity decreasing as frequency increases.

2. Simulation Model for Seabed Scholte Waves Excited by Sound Sources

2.1 Simulation Model

A seabed Scholte wave field finite element model is established using COMSOL multiphysics coupling software. The model comprises seawater and seabed sections using the acoustic-structure interaction time-domain module. Seawater employs pressure acoustic elements, the seabed uses solid mechanics elements, and the seabed interface is an acoustic-structure coupling boundary. A soft sound field boundary is set at the seawater surface, perfectly matched layers (PML) serve as absorbing boundaries on seawater sides, and low-reflection damping boundaries are applied to seabed sides and bottom. Water depth is 50 m, horizontal distance 1,500 m, and seabed depth 300 m. To reduce computational load, a 2D axisymmetric model simplifies the 3D problem, as shown in [FIGURE:4].

The pulsed source uses a low-frequency Ricker wavelet with 30 Hz dominant frequency [23], with waveform shown in [FIGURE:5].

2.2 Polarization of Seabed Scholte Waves

Polarization is characterized by ellipticity, which relates to the ellipse's major and minor axes. This study employs ellipticity to analyze polarization characteristics of Scholte wave particle motion trajectories.

Let l_1 be the sum of distances from any point on the ellipse to its two foci, used as an optimization parameter. For actual ellipse points:

$$l = \sum_{i=1}^{n-1} \sqrt{(x_i - a_1)^2 + (y_i - b_1)^2} + \sqrt{(x_i - a_2)^2 + (y_i - b_2)^2}$$

where (x , y) are coordinates on the ellipse, and (a_1, b_1) and (a_2, b_2) are the foci.

Variance is defined as:

$$S^2 = \sum (l - l_1)^2$$

where n is the total number of coordinates on the ellipse. Numerical simulation results optimize for minimum variance of l. Using the ellipse property l = 2a (where a is constant), the semi-major or semi-minor axis is obtained, and the other axis is derived from the focal length relationship. Ellipticity is then:

$$e = \pm \arctan(b/a)$$

where b is the semi-minor axis and a is the semi-major axis. Higher ellipticity values indicate more circular ellipses, while lower values indicate flatter ellipses. Thus, ellipticity characterizes Scholte wave particle motion trajectories, enabling investigation of polarization variation patterns.

3. Simulation Results and Discussion

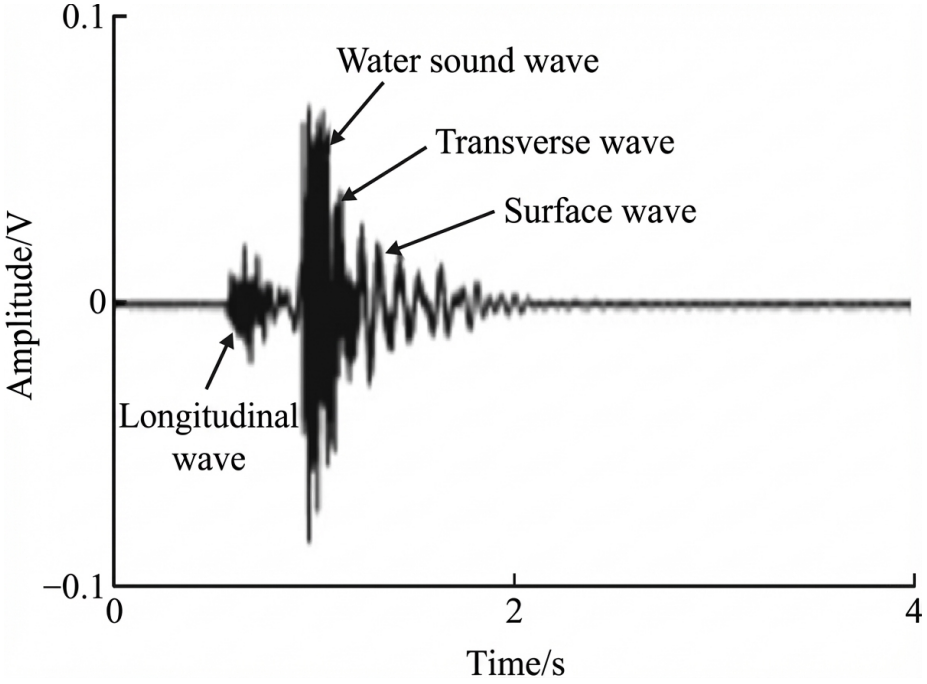

Figure 2: Figure 6

shows horizontal waveform curves at the fluid-solid interface 600 m from the source. To verify simulation accuracy, [FIGURE:7] presents seismic signal time-domain waveforms from reference [24]. Experimental results show P-waves, waterborne acoustic waves, S-waves, and surface waves—consistent with wave components obtained in this study. The simulation waveforms align well with experimental data, though waterborne acoustic signals are strongest in experiments due to greater energy and lower attenuation in real marine environments, plus multipath effects causing acoustic wave concentration. These results preliminarily validate the simulation.

Based on basalt parameters (P-wave velocity 4,500 m/s, S-wave velocity 1,900 m/s), P- and S-waves should arrive at 0.13 s and 0.32 s, respectively. Equation (7) yields a Scholte wave velocity of 1,448 m/s, corresponding to arrival at 0.41 s.

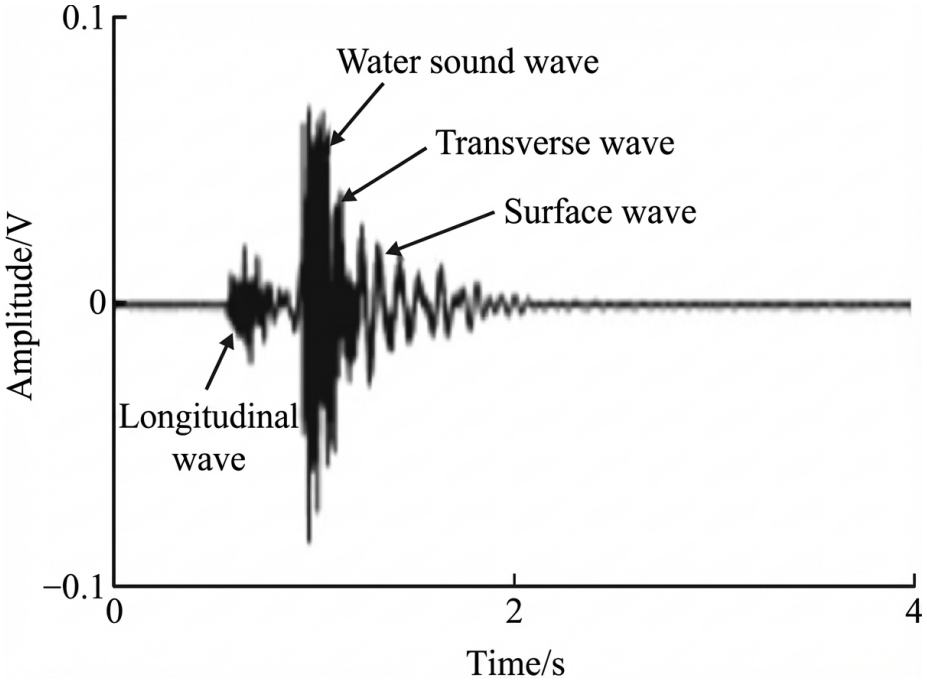

Figure 3: Figure 6

shows significant waveform differences around 0.54 s. The figure reveals arrays of P-waves, S-waves, and Scholte waves, with P-waves having the smallest horizontal velocity amplitude, followed by S-waves, and Scholte waves the largest. With increasing detection distance, Scholte waves attenuate slowest, offering potential for long-range target detection.

3.1 Dispersion and Polarization Characteristics of Scholte Waves Excited by Pulsed Sources Under Hard Seabed

Using basalt as the seabed medium, Scholte wave dispersion and polarization are analyzed. The pulsed source employs a 30 Hz Ricker wavelet.

For time-frequency analysis of pulsed source-excited Scholte waves, wavelet transform of the horizontal component yields the spectrogram in [FIGURE:8], where color intensity represents velocity amplitude (m/s), indicating signal strength variations across time and frequency. The highlighted region represents Scholte waves, whose frequency increases over time, stabilizing after 0.54 s—consistent with waveform differences observed in

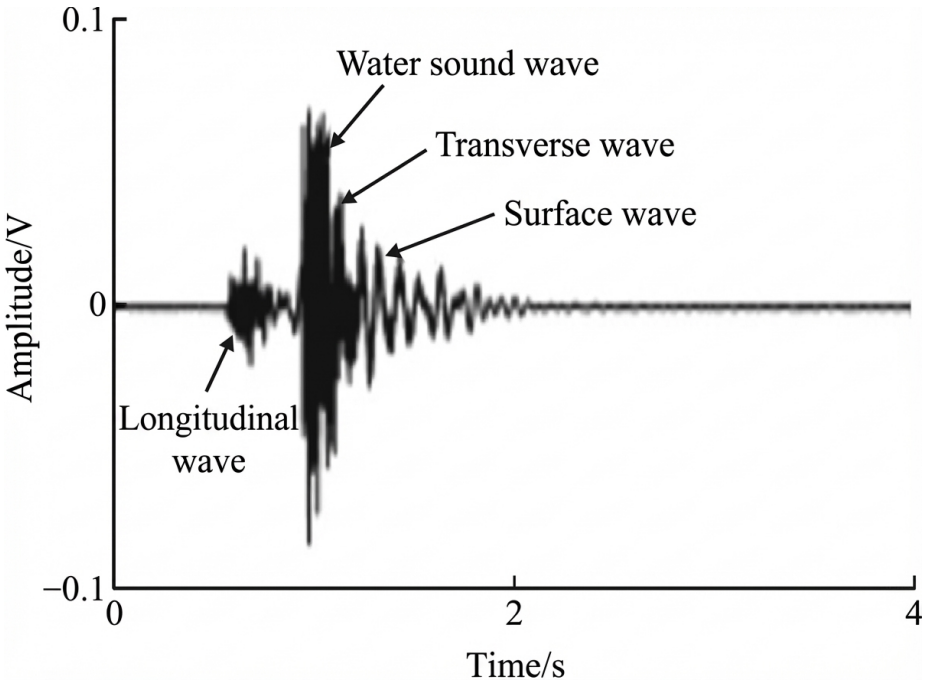

Figure 4: Figure 6

. This confirms that pulsed source-excited Scholte waves exhibit dispersion under hard seabed conditions; higher frequencies propagate slower, indicating that lower frequencies facilitate Scholte wave propagation.

Normalized horizontal and vertical waveform data from 0.41–0.54 s reveal Scholte wave polarization characteristics ([FIGURE:9]). The particle motion trajectory forms a counterclockwise ellipse [2], consistent with Scholte wave polarization properties and further validating result accuracy. Since Scholte wave polarization differs from P- and S-waves, polarization properties can distinguish Scholte waves from other wave types for further characteristic analysis.

3.2 Dispersion and Polarization Characteristics of Scholte Waves Excited by Pulsed Sources Under Soft Seabed

Using moraine as the seabed medium while keeping other conditions constant, [FIGURE:10] shows horizontal waveforms at 600 m from the source. With moraine parameters (P-wave 1,950 m/s, S-wave 600 m/s, water sound speed 1,500 m/s), P-waves arrive at 0.31 s, direct acoustic waves at 0.4 s, S-waves at 1.0 s, and Scholte waves (velocity 532 m/s from equation (7)) at 1.12 s. Unlike hard seabeds, the sequence shows P-waves, direct acoustic waves, S-waves, and Scholte waves, with direct acoustic waves having the largest horizontal velocity amplitude and Scholte waves the smallest—indicating that soft seabeds are less favorable for Scholte wave excitation.

Wavelet transform of the horizontal component yields the spectrogram in [FIGURE:11]. The highlighted region shows direct acoustic waves, which dominate over weak Scholte wave signals, making dispersion phenomena difficult to observe—demonstrating that soft seabeds hinder observation of pulsed source-excited Scholte wave dispersion.

3.3 Dispersion and Polarization Characteristics of Scholte Waves Excited by Continuous Sources Under Hard Seabed

Using basalt as the seabed medium, a 30 Hz sinusoidal wave serves as the continuous source [23].

For dispersion characteristics, [FIGURE:12] shows the spectrogram from wavelet transform of the horizontal component at 600 m from the source. Due to continuous excitation, Scholte waves at the fluid-solid interface are persistently generated. Before 2.5 s, various acoustic waves superimpose; after 2.5 s, Scholte waves stabilize. Scholte waves exhibit a cutoff frequency, with propagation velocity decreasing as frequency increases before stabilizing—consistent with theoretical dispersion characteristics. This confirms that continuously excited Scholte waves show dispersion that can be continuously observed.

[FIGURE:13] shows particle motion trajectories at 600 m, revealing stable counterclockwise elliptical motion. Ellipticity variation over time is shown in [FIGURE:16] (hard seabed). Continuous excitation maintains stable ellipticity, while pulsed excitation shows initial decrease followed by increase. Because Scholte waves are continuously generated at the interface, ellipticity eventually stabilizes under continuous sources, whereas pulsed sources exhibit decreasing

then increasing ellipticity as Scholte waves attenuate. These differences provide preliminary criteria for detecting the two underwater source types.

3.4 Dispersion and Polarization Characteristics of Scholte Waves Excited by Continuous Sources Under Soft Seabed

Using moraine as the seabed medium, [FIGURE:14] shows the spectrogram at 600 m from the source. Compared with hard seabeds, Scholte waves stabilize earlier because soft seabeds generate weaker signals with less fluctuation, reaching stability faster over time. Since Scholte wave signal strength is comparable to direct acoustic waves, dispersion can be continuously observed in the spectrogram.

[FIGURE:15] shows stable counterclockwise elliptical particle motion trajectories at 600 m, with larger ellipticity than under hard seabed conditions. Ellipticity variation is shown in [FIGURE:16] (soft seabed).

Based on particle motion trajectories, Scholte waves under hard seabeds exhibit predominantly vertical vibration for both source types, while under soft seabeds, continuously excited Scholte waves show horizontal vibration—facilitating horizontal propagation.

Conclusions

This study investigated dispersion and polarization characteristics of Scholte waves excited by pulsed and continuous point sources in shallow seas. Based on normal mode theory, dispersion characteristics were analyzed, and time-domain finite element modeling combined with wavelet transform examined dispersion and polarization of particle motion trajectories. Main conclusions are:

1) In the shallow-water semi-infinite elastic seabed model, Scholte waves can be excited under both hard and soft seabed conditions, exhibiting dispersion phenomena.

2) Under hard seabeds, dispersion is observable for both source types in spectrograms. Under soft seabeds, direct acoustic waves dominate over weak Scholte wave signals, making pulsed source-excited Scholte wave dispersion difficult to observe, while continuous source conditions allow dispersion observation due to comparable signal strengths.

3) Particle motion trajectories differ significantly between source types: pulsed sources produce ellipticity that first decreases then increases, while continuous sources maintain stable ellipticity. This difference provides preliminary criteria for detecting the two underwater source types. Under hard seabeds, both source types generate vertically dominated Scholte waves, whereas under soft seabeds, continuously excited Scholte waves are horizontally dominated, favoring horizontal propagation.

References

[1] SI Jiege, FENG Haixin, SU Jun, et al. Research on shallow sea detection technology based on seismic wave[J]. *Progress in geophysics*, 2022, 37(6): 2596-2603 (in Chinese).

[2] RAUCH D. Experimental and theoretical studies of seismic interface waves in coastal waters[M]//KUPERMAN W A, JENSEN F B. *Bottom-Interacting Ocean Acoustics*. Boston, MA: Springer US, 1980: 307-327.

[3] FRIVIK S A, HOVEM J M. Determination of shear wave properties in the upper seafloor using seismo-acoustic interface waves[C]//IEEE Oceanic Engineering Society. *OCEANS'98. Conference Proceedings*. Piscataway, NJ, USA: IEEE, 1998: 682-686.

[4] GIARD J L, POTTY G R, MILLER J H, et al. Validation of an inversion scheme for shear wave speed using Scholte wave dispersion[C]//2013 OCEANS-San Diego. Piscataway, NJ, USA: IEEE, 2013: 1-9.

[5] DU S Y, CAO J P, ZHOU S H, et al. Observation and inversion of very-low-frequency seismo-acoustic fields in the South China Sea[J]. *The Journal of the Acoustical Society of America*, 2020, 148(6): 3992-4001.

[6] EWING M, VINE A, WORZEL J L. Photography of the ocean bottom[J]. *Journal of the optical society of america*, 1946, 36(6): 307-327.

[7] RAUCH D. Seismic interface waves in coastal waters: a review[J]. *Seismic interface waves in coastal waters: a review NATO*, 1980, 5(1): 1-106.

[8] SHAO Yuxin, LI Huan, ZHANG Zipu, et al. Research on recognition of Scholte wave in shallow sea ship seismic wave[J]. *Journal of Shenyang Ligong University*, 2017, 36(3): 32-37 (in Chinese).

[9] VINH P C. Scholte-wave velocity formulae[J]. *Wave motion*, 2013, 50(2): 180-190.

[10] ZHU Hanhao, ZHENG Hong, LIN Jianmin, et al. Influence of ocean environment parameters on Scholte wave[J]. *Journal of Shanghai Jiao Tong University*, 2016, 50(2): 257-264 (in Chinese).

[11] QIU H M, XIA T D, CHEN W Y, et al. Low-frequency pseudo-Rayleigh and pseudo-Scholte waves at an interface of liquid/soft porous sediment with underlying hard porous sediment substrate[J]. *Geophysical journal international*, 2019, 219(1): 540-552.

[12] FLORES-MENDEZ E, CARBAJAL-ROMERO M, FLORES-GUZMÁN N, et al. Rayleigh's, Stoneley's, and Scholte's interface waves in elastic models using a boundary element method[J]. *Journal of applied mathematics*, 2012, 2012(1): 313207.

[13] WANG Q L, ZHU H H, TANG Y F, et al. Propagation characteristics of low-frequency acoustic wave in full waveguide of shallow water based on time-domain

finite element method[J]. *IOP conference series: earth and environmental science*, 2021, 734(1): 012038.

[14] ZHAO S, ZHANG J, WANG Z L, et al. Improving Scholte-wave vibration signal recognition based on polarization characteristics in coastal waters[J]. *Journal of coastal research*, 2020, 36(2): 382-389.

[15] TOMAR G, SHAPIRO N M, MORDRET A, et al. Radial anisotropy in Valhall: ambient noise-based studies of Scholte and Love waves[J]. *Geophysical journal international*, 2017, 208(3): 1524-1539.

[16] WANG Bo, ZENG Linfeng, ZHANG Yan, et al. Time-frequency domain polarization analysis of seismic waves in the whole space of mine and its experimental study[J]. *Journal of China Coal Society*, 2022, 47(8): 2978-2984 (in Chinese).

[17] ZHAO Han. Research on key technologies of very low frequency underwater acoustic and seismic wave joint detection[D]. Hangzhou: Zhejiang University, 2018.

[18] LU J, WANG Y, CHEN J Y. Noise attenuation based on wave vector characteristics[J]. *Applied sciences*, 2018, 8(5): 672.

[19] HUANG L Y, WANG S C, SONG X J. Comparison study of three-component polarization analysis methods for seismic advanced detection in the roadway[J]. *Arabian journal of geosciences*, 2020, 13(23): 1276.

[20] HAN Xue. Analysis and application research of ship seismic wave signal characteristics[D]. Harbin: Harbin Engineering University, 2010.

[21] ZHANG Haigang. Research on modeling and propagation 规律 of very low frequency sound in shallow sea[D]. Harbin: Harbin Engineering University, 2020.

[22] ZHAO S, ZHANG J, GUO C A, et al. Study on fluctuant element and attenuation rules of seismo-acoustic wave[J]. *Noise & vibration worldwide*, 2019, 50(7): 217-226.

[23] LUO Xiayun, MENG Luwen, CHENG Guangli, et al. A study on frequency characteristics of Scholte wave excited by sound sources in a shallow sea[J]. *Journal of vibration and shock*, 2020, 39(16): 267-274 (in Chinese).

[24] DIAO Aimin, CHENG Guangli, WANG Zeming. On the dispersive characteristics of shallow water seismic waves excited by air gun sound source in shallow water[J]. *Journal of Northwestern Polytechnical University*, 2019, 37(4): 724-729 (in Chinese).

(Edited by ZHANG Lu)